INTERNATIONAL JOURNAL OF CLIMATOLOGY
Int. J. Climatol. **27**: 979–988 (2007)
Published online 6 December 2006 in Wiley InterScience
(www.interscience.wiley.com) DOI: 10.1002/joc.1454

RMetS
ROYAL METEOROLOGICAL SOCIETY

Detecting trends in tropical rainfall characteristics, 1979–2003†

K.-M. Lau* and H.-T. Wu‡
Laboratory for Atmospheres NASA/Goddard Space Flight Center Greenbelt, MD 20771, USA

Abstract:

Analyses of two state-of-the-art, blended space-based and ground-based global rainfall data sets from the Global Precipitation Climatology Project (GPCP) and the Climate Prediction Center Merged Analysis Product (CMAP) reveal that there was a significant shift in the probability distribution functions of tropical rainfall during the period 1979–2003. This shift features a positive trend in the occurrence of heavy (top 10% by rain amount) and light (bottom 5%) rain events in the tropics during 1979–2003 and a negative trend in moderate (25–75%) rain events. These trends are consistent in both data sets and are in overall agreement with the Climate Research Unit's (CRU) gauge-only rainfall data over land. The relationships among the trends and the possible long-term changes in rainfall characteristics are discussed. Published in 2006 by John Wiley & Sons, Ltd.

KEY WORDS tropical rainfall; trend; extreme

Received 2 May 2006; Revised 25 August 2006; Accepted 24 September 2006

INTRODUCTION

All water that sustains human life ultimately comes from precipitation. Latent heating from precipitation is the main driver of the atmospheric water cycle, which strongly influences the Earth's weather and climate. Yet, in spite of the well-documented rapid rise in global temperature in the last century, there has been no clear evidence of long-term change in global precipitation (IPCC, 2001; Karl and Trenberth, 2003; Allen and Ingram, 2002). Recent studies have shown that there has been a significant increase in precipitation over land at high-latitudes since the 1950s, and a possible increase over tropical oceans but reduction over tropical land (New *et al*., 2001; Kumar *et al*., 2003; Bosilovich *et al*., 2005). Over the oceans, where rainfall estimates rely on satellite observations, the uncertainty in the estimate of total rainfall is large. Since about two-third of the world is covered by oceans, the lack of reliable oceanic rainfall estimates for long-term signal detection is a reason that the trend in global rainfall associated with climate change, if present, has not been identified.

A more fundamental reason for not detecting long-term global rainfall trend is that rainfall is a chaotic quantity governed by nonequilibrium atmospheric dynamics and convection, in contrast to temperature, which is a state variable that is subject to equilibrium thermodynamic controls. This is evident in the intrinsically small scale and noisy nature of rainfall, and hence the relatively low signal-to-noise ratio in climate detection. Globally, the release of latent heat from enhanced convection and increased rainfall in one region has to be balanced by radiative cooling, both locally and in remote regions, with compensating subsidence and suppressed rainfall. This means that in response to long-term climate forcing, the global water cycle is likely to adjust not only dynamically but also structurally, as reflected by the changes in rainfall characteristics, such as frequency of occurrence of intense events, persistence of wet and dry spells, and changes in relative abundance of cold *versus* warm rains and high *versus* low cloud types (New *et al*., 2001; Meehl *et al*., 2000; Weilicki *et al*., 2002; Lau and Wu, 2003; Lau *et al*., 2005). Because of the large compensation, the trend in global total rainfall is likely to be relatively small and probably within data errors. Even with the recent advances in space-based rainfall measurements from the Tropical Rainfall Measuring Mission (TRMM), and reconstruction of the state-of-the-art global data sets merging satellite and rain gauge observations, estimating global rain amounts remains a major challenge.

In this study, we adopt a new approach for detecting changes in long-term rainfall using existing data, based on the premise that (1) a shift in rainfall probability distribution function (PDF) associated with changing rainfall characteristics is likely to be more sensitive to climate change than the global mean total rain amount, and hence would be more detectable, and (2) current multi-decadal merged satellite-gauge rainfall products contain useful information on long-term changes in

* Correspondence to: K.-M. Lau, Laboratory for Atmospheres, Code 613, Building 33, Rm C121, NASA Goddard Space Flight Center, Greenbelt, MD 20771, USA. E-mail: william.k.lau@nasa.gov
† This article is a US Government work and is in the public domain in the USA
‡ Science and Systems Application Inc., Lanham, Maryland

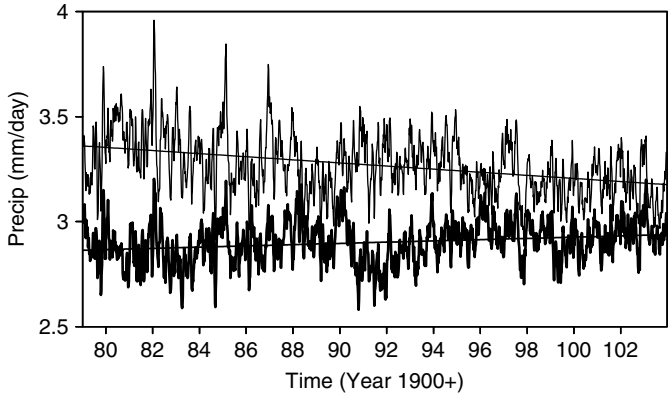

Figure 1. Time series of pentad GPCP (thick line) and CMAP (thin line) tropical mean rainfall from 1979–2003. A 30-day running mean filter has been applied to both data sets. The straight lines are obtained from the linear regression based on each data set.

rain characteristics, even though they may differ in the estimate of the trend in total rain amount. We will focus on tropical rainfall because that is where most of the global rainfall occurs, and because tropical rainfall estimates have seen significant improvements in the last decade and will continue to improve in the next decade owing to NASA's commitment to TRMM and the Global Precipitation Mission (GPM).

DATA DESCRIPTION

For this study, we employ two widely used long-term (1979-present) global precipitation products: the Global Precipitation Climatology Project (GPCP), and the Climate Prediction Center (CPC) merged analysis of precipitation (CMAP). Both have monthly and pentad products derived from a mix of satellite estimates over ocean and land and rain gauge measurements from land and atolls, although the input data and blending methodologies of the two differ considerably (e.g. Adler *et al*., 2003; Xie *et al*., 2003; Yin *et al*., 2004). We elect to use the GPCP and CMAP pentad products to allow for more samples to define rainfall characteristics. The pentad CMAP data are produced similar to the monthly CMAP, but include daily data inputs. The pentad GPCP is derived from the pentad CMAP, but is additionally adjusted to the monthly GPCP-merged analysis and therefore has the same long-term mean properties as the monthly GPCP (Adler *et al*., 2003; Xie *et al*., 2003). For this work, it is important to recognize that, because of similar data sources, both data sets are not entirely independent and that both suffer from systematic bias and uncertainties stemming from the use of multiple satellites and different retrieval algorithms (Xie *et al*., 2003). Yet these are the only two long-term global data sets presently available. *In spite of the differences between the two data sets in total rain accumulation,* we shall be using these data sets to determine whether we can detect a consistent long-term *qualitative* shift in the rainfall PDF, and whether such a shift is amenable to plausible physical interpretations (see section 'Physical Interpretation'). This work is focused on using a new approach to extract useful climate information from the data set with known quantitative discrepancies. We defer to rainfall retrieval and data experts the important tasks of further improvement and re-processing of these two data sets, which are extremely important for reducing uncertainties in the quantitative trend analysis. For cross checking the results (over land), we use the long-term Hadley Centre Climate Research Unit's (CRU) Time Series 2.0 global gridded land precipitation products (New *et al*., 2000).

RESULTS

We define a trend empirically as the linear regression fitted to the data for the period 1979–2003. We caution that this definition does not necessarily imply a 'real trend' in the sense of the long-term climate change time scale (>century). Here, the trend only represents a monotonic shift, which may be part of a multi-decadal signal that is present in the data records.

Preliminary analysis

Figure 1 shows the time history of tropical (30 °S–30 °N) mean pentad rainfall for GPCP and CMAP. A 30-day running mean has been applied to both data sets to emphasize the low-frequency variability. The discrepancy between GPCP and CMAP is obvious. The long-term (1979–2003) mean rainfall of GPCP (2.9 mm day^{-1}) is significantly smaller than that of CMAP (3.3 mm day^{-1}). CMAP shows a clear negative trend compared with GPCP, which shows a slight positive trend. The trend found in CMAP is likely to be contaminated by artifacts due to discontinuity in the inclusion of special sensor microwave/imager (SSM/I) data after 1987 and a change in quality of the atoll data after 1996 (Yin *et al*., 2004). These account for the shift in the apparent rainfall variability before and after 1987 and the closer agreement between CMAP and GPCP after 1996 (GPCP does not use atoll data). Despite the systematic bias and differences in the trend, both data sets capture the major rainfall peaks associated with El Niño, e.g. 1982, 1985, 1987, 1997, and exhibit strong interannual

Published in 2006 by John Wiley & Sons, Ltd.

DOI: 10.1002/joc

and some interdecadal variations, albeit with different phases. Comparing with standard TRMM rainfall products (not shown), we also note that the systematic bias between the tropical mean GPCP and CMAP is comparable to that between Version 5 and Version 6 of the TRMM rainfall data. Thus, the global trend in total rainfall, if present at all, is most likely to be within the data error of current satellite estimates. Clearly, in order to extract useful information on long-term changes in rainfall, it is necessary to go beyond the comparison of global trends in total rainfall.

As a first step in our new approach, we examine the changes in extreme rain events. We bin the rainfall data according to rain rates at 1 mm day^{-1} interval and calculate the accumulated rain amount contributed by each rain bin for the tropics for both GPCP and CMAP. We then define light rain as the category of rain at the lowest 5% accumulated rain amount (B5), heavy rain as that at the top 10% (T10), and rainfall within the inter-quartile range as the intermediate rain (I25). From Table I, it is evident that GPCP and CMAP describe similar rain characteristics with the same threshold value (=1 mm day^{-1}) for B5. The range for I25 and the threshold for T10 are smaller for GPCP compared to that for CMAP, which is consistent with the smaller mean value of GPCP shown in Figure 1.

It is noted that light rain estimate is more sensitive to measurement error (Olson *et al*., 2006). Our calculation of the error field associated with the pentad CMAP B5 rain yields a mean error of 0.19 mm day^{-1} (approximately 1/5 of our 1 mm day^{-1} threshold for B5 rain) for the tropical region. The estimated error of GPCP rain is expected to be even smaller than that of CMAP (Xie *et al*., 2003). Hence the B5 threshold is large enough compared to the mean error for this category of rain but still small enough to separate the light rain events from moderate rain.

Table I. Threshold rain rate, climatological rain amount, frequency of occurrence (FOC), and linear change (mm) over 25 years (1979–2003) averaged over the tropics for light, intermediate, and heavy rain, which are defined as the bottom 5% (B5), inter-quartile range (I25), and top 10% (T10), respectively, for (A) GPCP and (B) CMAP.

(A) GPCP

	B5	I25	T10
Threshold rain rate (mm day^{-1})	<1	(4, 14)	>20
Mean amount (mm)	46	544	119
Linear change in amount (mm)	3.8	−55	81
FOC (%)	38	20	1.3
Linear change in FOC (%)	9.4	−2.2	0.8

(B) CMAP

	B5	I25	T10
Threshold rain rate (mm day^{-1})	<1	(4, 16)	>23
Mean amount (mm)	49	630	133
Linear change in amount (mm)	4.2	−88	44
FOC (%)	39	22	1.2
Linear change in FOC (%)	4.2	−3	0.3

Figure 2 shows the time series of the yearly accumulated rain amount averaged over the tropics, and the frequency of occurrence (FOC) for the light and heavy rain, respectively. Here, FOC is defined by the ratio of the occurrences of each 5-day rain rate at any 2.5° grid box residing in a particular rain bin to the total counts of rain occurrences over the tropics. In contrast to the total rainfall, both the GPCP and CMAP data indicate clear positive trends in both rain amount and FOC of light and heavy rain categories. Note that the trends in both light and heavy rains are more prominent after 1986, indicating that they are not due to the inclusion of SSM/I data. The linear trend estimates exceed the 99% confidence level (statistically significant at the 1% level) on the basis of the R^2-test (Wilks, 1995). Table I shows that, for light rain in the tropics, the long-term (25 year) annual mean accumulation is approximately 46 mm for GPCP and 49 mm for CMAP. Both show an increase in annual rainfall of about 4 mm over 25 years. The corresponding increase in FOC for light rain is substantial, approximately 9% for GPCP and 4% for CMAP. The increase in annual rainfall in the heavy rain category is quite large, estimated to be around 81 mm for GPCP and 44 mm for CMAP over 25 years. The positive trend in the FOC of heavy rain (Figure 2(D)) is also evident in both data sets. It is important to note that heavy rain events are relatively rare, as indicated by the FOC range of 0.8–1.8% (Figure 2(D)), and that light rains occur much more frequently and are widely spread, as is evident in the 33–45% FOC range (Figure 2(B)). The physical implication of this difference on the water and energy balance of the tropics will be discussed in the section'Physical Interpretation'.

Probability distribution function (PDF)

The preliminary trend analysis for extreme rainfall categories suggests that there may be a shift in the rainfall PDF during the data period. To examine such a shift, we construct the climatological rainfall PDF for the tropics for both GPCP and CMAP and then compute, by linear regression, the trend for each binned rain rate. To ensure that the PDF and the estimated trend are not sensitive to the data period, we have computed them for the entire data period and for the post-SSM/I era (1988–2003). The results are qualitatively similar. Henceforth, we only show results for the entire period (1979–2003). The climatological PDFs of the GPCP and CMAP rainfall and FOC are shown in Figures 3(A) and (B), respectively. Compared to GPCP, CMAP overestimates rainfall in all categories, but maintains a very similar PDF structure (Figure 3(A)). Both PDFs show a maximum at the intermediate range of ∼3–7 mm day^{-1}. The GPCP PDF tails off toward high rain rates slightly faster than CMAP. The FOC PDFs (Figure 3(B)) of GPCP and

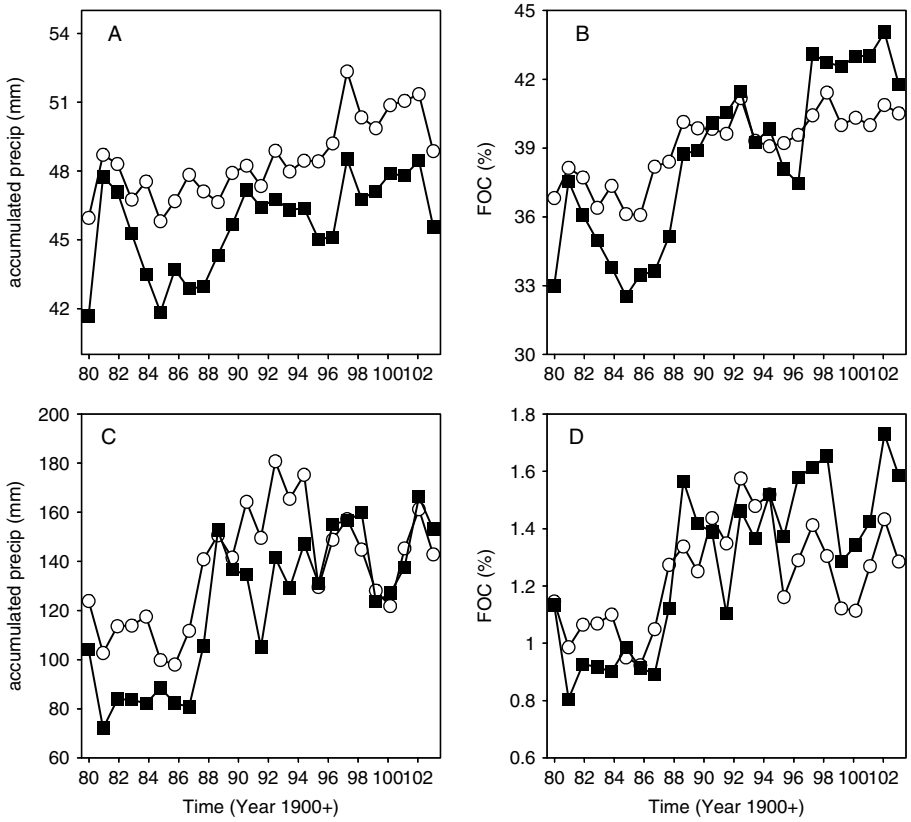

Figure 2. Time series of (A) yearly accumulated precipitation amount and (B) frequency of occurrence (FOC) for light rain (bottom 5% by precipitation amount), and similar data (C and D) for heavy rain (top 10% by rain amount), for GPCP (closed squares) and CMAP (open circles), respectively.

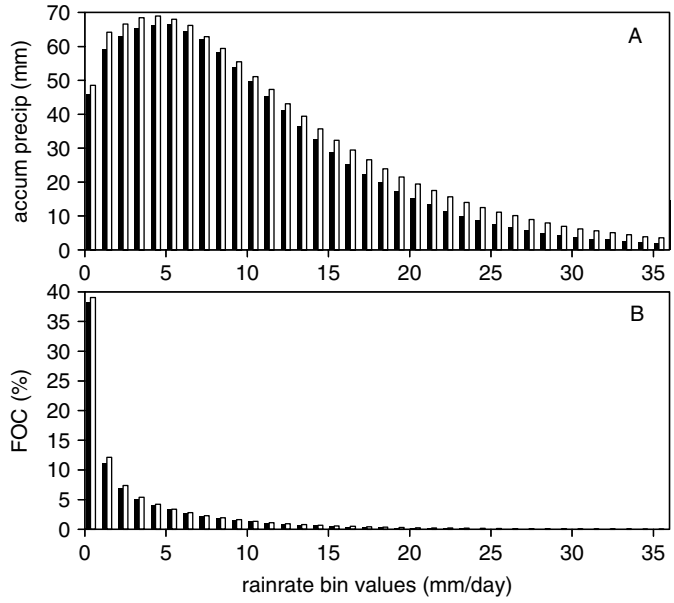

Figure 3. The climatological (1979–2003) PDF for (A) yearly accumulated precipitation amount, and (B) FOC; for GPCP (solid bar) and CMAP (outlined bar), respectively.

CMAP agree well with each other, showing that B5 occurs far more frequently (~40%) compared to all other rain events. The geographic distribution of FOC for each rain category also shows reasonable agreement between the two data sets. As shown in Figure 4, B5 rain is found over large expanses of the subtropical ocean with relatively low sea-surface temperature, i.e. the eastern Pacific, the eastern Atlantic, and the southeastern Indian Ocean, with frequent occurrences off the west coast of the continents, most likely in conjunction with

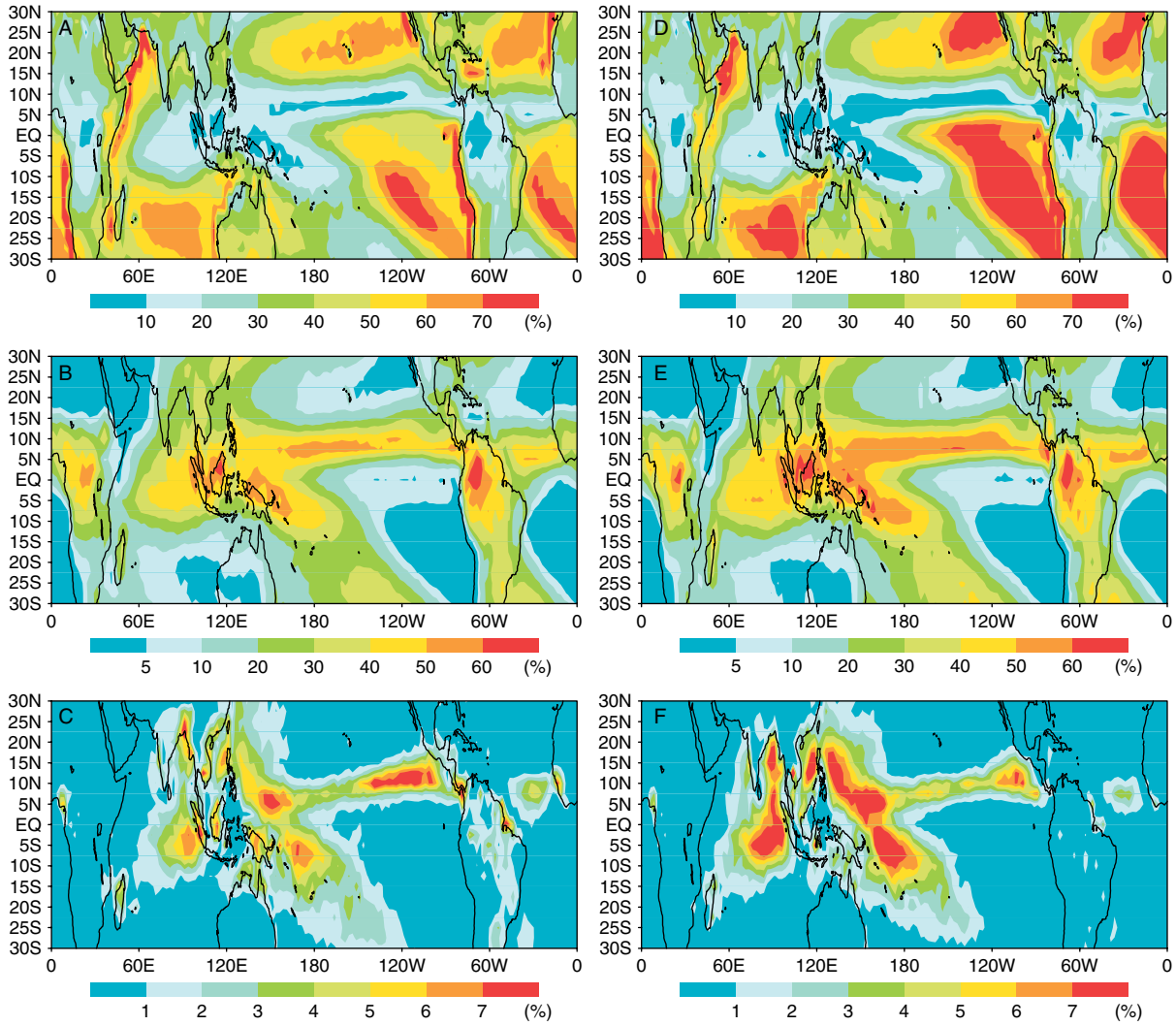

Figure 4. Geographic distribution of FOC for (A) B5, (B) I25, and (C) T10 for GPCP and (D) B5, (E) I25, and (F) T10 for CMAP.

coastal upwelling and stratocumulus clouds. I25 rain is found most frequently in the tropical warm pool regions, with strong signals over the land masses of central and western Africa, the maritime continent, and Amazonia. T10 rain is found predominantly over the core convective region of the western Pacific, eastern Indian Ocean, and the Pacific and Atlantic intertropical convergence zone (ITCZ).

To quantify the shift of the rainfall PDF, we follow the same procedure to compute the trend of rain amount and FOC over the entire tropics (30°S–30°N) binned by rain rates. Figures 5(A) and (B) show the linear trend increment of rain amount and FOC over the 25 year period, with the data binned at the interval of 1 mm day^{-1}. Only trends that exceed the 95% confidence level are shown. Both PDFs show significant positive trends in B5 and T10, with a very pronounced reduction in I25. The negative trend in GPCP is prevalent for rain rates >1 mm day^{-1} and up to 14–15 mm day^{-1}, while the negative trend in CMAP extends further to rain rates up to 20 mm day^{-1}. This larger range of rain rates with negative trend in CMAP, compared to the smaller range in GPCP, helps explain the negative trend of the total rain amount observed in the CMAP data, but not in GPCP (Figure 1).

The change from a positive trend in the first rain bin (B5) to a negative trend in the second rain bin implies a transition zone of near zero trend for rain events with rain rate around 1 mm day^{-1}. As stated previously, the 1-mm day^{-1} threshold is significantly above the measurement error of 0.19 mm day^{-1}. We test the stability of the trends as a function of bin size using a smaller rain bin interval (1/3 mm day^{-1}) for light and moderate rains that have high FOC. Our analyses confirm such stability, showing a positive trend for the first two bins (0–0.66 mm day^{-1}), insignificant trend for the transition bins (0.67–1.33 mm day^{-1}), and a negative trend for the rest of the light to moderate rain bins.

The increase in FOC (Figure 5(B)) of B5 is very pronounced in both data sets, with GPCP showing more than 9% increase and CMAP showing more than 4% increase. Similarly, the reduction in the FOC of I25 is also very clear. In contrast, the increase in FOC in T10 is barely noticeable in Figure 5(B) because of the extremely

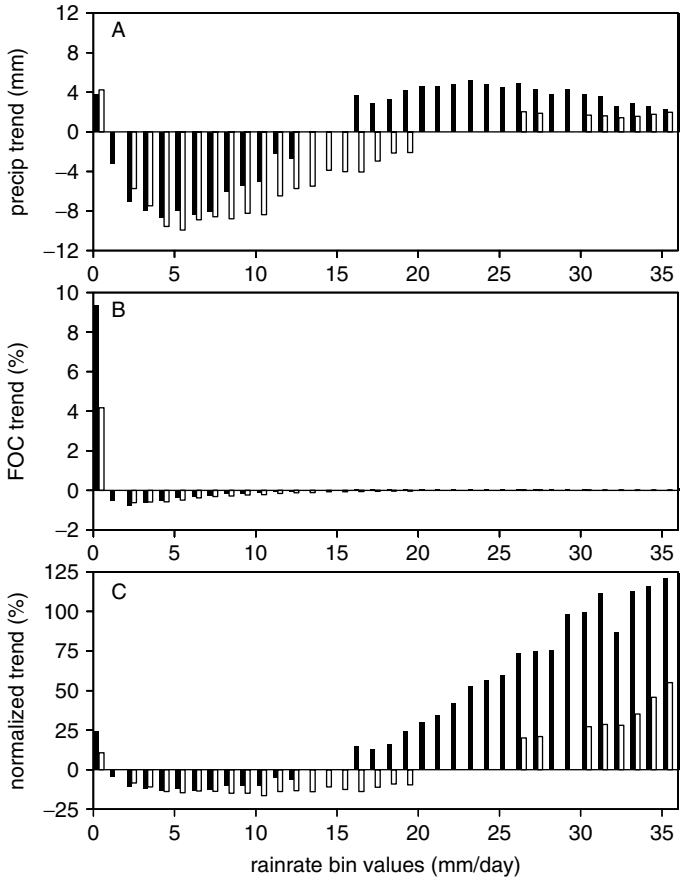

Figure 5. Shift in PDF shown as linear trend increment over 25 years as a function of rain rate for (A) yearly accumulated precipitation amount, (B) FOC, and (C) same as in (B) except being normalized by the mean in each rain rate bin; for GPCP (solid bar) and CMAP (outlined bar), respectively.

low FOC compared to those of B5 and I25. However, in terms of fractional increments (normalized by the climatological mean for each rain rate bin), the trend in FOC becomes substantial in all three categories, and most pronounced in T10 (Figure 5(C)). It is clear that the more extreme the rain rate, the stronger is the fractional increment signal, indicating that the most intense rain systems are the most affected by the trend.

Spatial pattern of trends

We examine the spatial distributions of the linear trend increments for B5, T10, I25, and total rainfall in this subsection. Here, the increments are computed as the accumulated rainfall for 1991–2002 minus that for 1979–1990, separately for GPCP and CMAP. Since the two data sets show qualitatively similar spatial distributions, only those of GPCP are shown in Figure 6 to focus the discussion.

Figure 6(A) shows that, in the recent decade (1991–2002) compared to the previous one (1979–1990), there is a somewhat uniform increase in B5 rainfall over all tropical oceans, with noticeable reduction in the areas off the west coast of the continents, the subtropical continental regions, and the maritime continent. In agreement with the PDF analysis shown previously, I25 (Figure 6(B)) shows reduction over a wide swath of the tropical oceans, in the broad regions encompassing the Pacific and Atlantic ITCZ, the subtropics, and the eastern Indian Ocean. Exceptions are found over the maritime continent and northwestern South America, where I25 is enhanced. As stated, B5 rain is actually found to decrease over the maritime continent. Hence the opposite polarity of long-term trend between B5 and I25 appears to hold over the maritime continent as well. Figure 6(B) also shows a large negative trend over the equatorial central Africa. This trend is also found in CMAP (not shown), but is not observed in the analysis of the CRU data (see subsection 'Comparison with independent data').

The trend pattern in Figure 6(C) shows that T10 rainfall over the tropical oceans generally increases over the decades, consistent with the PDF shift. The most pronounced positive trends are found in the deep convective cores in the ITCZ and the South Pacific Convergence Zone (SPCZ), and also in the land-anchored monsoon depressions. Substantial reductions in T10 are found over the maritime continent, equatorial central America, and northeastern Brazil, and to a lesser extent over central Africa. The concentrated regions of large positive and negative anomalies reflect the centers of rising and sinking motions of an anomalous Walker circulation. This feature is also evident in the total rainfall trend (Figure 6(D)). However, in comparison to the total

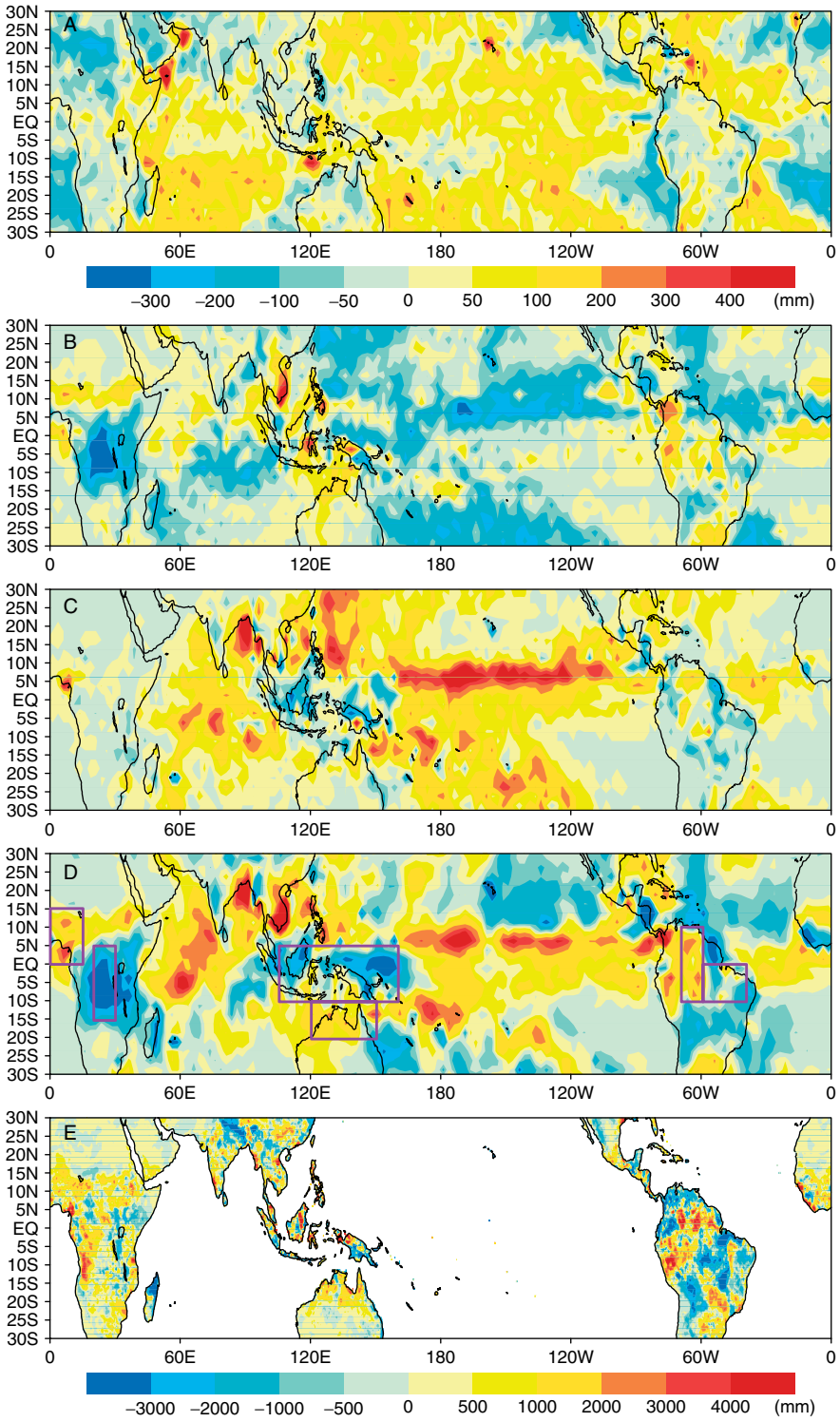

Figure 6. Difference patterns (1991–2002 minus 1979–1990) showing quasi-decadal shift in accumulated precipitation amount for (A) B5, (B) I25, (C) T10, and (D) total rainfall for GPCP and (E) total rainfall for CRU.

rainfall trend (Figure 6(D)), it is clear that each of the major rain categories shows a more uniform increase or decrease over the entire tropical oceans, indicating a substantial change in the large-scale circulation, *as well as a change in the rainfall characteristic*s, associated with a long-term large-scale adjustment in the tropical water cycle (see section'Physical Interpretation').

Comparison with independent data

In this subsection, we seek corroboration of our results with an independent long-term rainfall data set. Since there is no other independent long-term rainfall data set over the open oceans, besides GPCP and CMAP, we can only compare our results with the CRU rainfall, which is based solely on rain gauge data over land. We note that

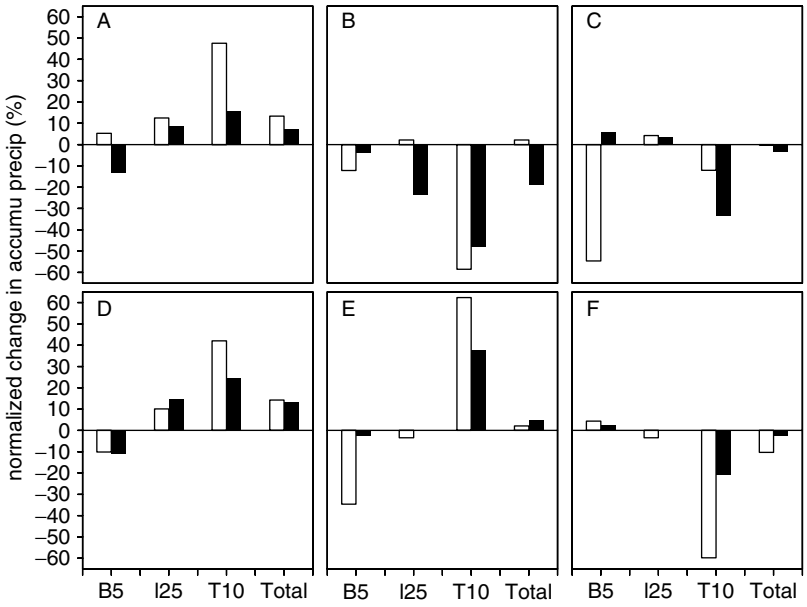

Figure 7. Normalized change in area-averaged accumulated precipitation between the periods 1979–1990 and 1991–2002 in B5, I25, T10, and total rainfall, for (A) West African monsoon region (0–15 °N, 0–15 °E), (B) equatorial central Africa (15 °S–5 °N, 20 °E–30 °E), (C) maritime continent [10 °S–5 °N, 105 °E–160 °E], (D) northern Australia [20 °S–10 °S, 120 °E–150 °E], (E) equatorial western South America [10 °S–10 °N, 70 °W–60 °W], and (F) equatorial eastern South America [10 °S–0, 60 °W–40 °W], for GPCP (solid bar) and CRU (outlined bar), respectively. Here, the rain rate ranges for B5, I25, and T10 are defined on the basis of rainfall over tropical land only.

the atoll data were used to determine the error structure in constructing the pentad GPCP and CMAP data and that they may also have a sampling problem before and after 1996 (Xie *et al*., 2003; Yin *et al*., 2004), they are therefore not appropriate for trend comparison. Because of different spatial and temporal scales between the GPCP (pentad, 2.5 × 2.5 degree spatial resolution) and CRU (monthly, 0.5 × 0.5 degree spatial resolution), the comparison presented here is rather crude. Figure 6(E) shows the spatial distribution of the change (1991–2002 minus 1979–1990) in CRU rainfall. Similarities in the large-scale pattern between the CRU and the GPCP (Figure 6(D)) can be discerned, particularly over tropical South America, regions in South Asia, and equatorial Africa. The magnitudes of the anomalies differ between the two data sets, in part due to the different spatial and temporal resolutions and in part due to the fundamental differences in the satellite rainfall estimates compared to the rain gauge observations (Nesbitt *et al*., 2004). As noted, the negative anomaly over equatorial Africa seems to be excessive for GPCP compared to CRU.

To further quantify the comparison, we select large land regions between 20 °S and 15°N (shown as rectangles in Figure 6(D)), where there are pronounced anomalies on the basis of GPCP. We then compute the fractional change in rainfall amount (1991–2002 minus 1979–1990) with respect to each rain category (B5, I25 and T10) and for total rain over the regions for GPCP and for CRU, respectively (Figure 7). Note that the fractional change of total rainfall is relatively small (∼10–15%), having the same sign in both data sets in all regions, except for equatorial central Africa (Figure 7(B)). The fractional change is largest (∼20–50%) in T10 and is consistent between the two data sets in all the selected regions. The fractional changes in I25 and in B5 are usually smaller and less consistent among the two data sets. The magnitude of the rainfall change due to B5 is much smaller than that due to I25 and T10 (Figure 6). On the other hand, the absolute change in I25 rain amount is comparable to that of T10 in both data sets. Since the trends of T10 and I25 tend to be opposite in sign and comparable in magnitude (as shown in Figures 6(C) and (D)), the total rainfall trend appears as a small difference between two large terms, and hence it is very sensitive to the errors in the estimated trend. In regions where the two data sets disagree in total rainfall trend, for example, over equatorial central Africa (Figure 7(B)), CRU depicts a small positive trend in total rainfall and in I25, but GPCP shows the opposite trend, even though their trends agree in T10. An examination of the time series of rainfall over equatorial central Africa (not shown) indicates that the large decrease in GPCP total rainfall (mostly due to I25) stems from a major negative shift since 1987, suggesting the possibility that the decrease may be an artifact related to the inclusion of the SSM/I data, which may have adversely impacted the land rainfall estimate in GPCP over Africa. Over the maritime continent (Figure 7(C)), CRU shows negligible fractional changes in total rainfall, yet GPCP shows a small negative fractional change. However, both data sets are consistent in showing a strong fractional reduction in T10 and an increase in I25, though the magnitudes differ considerably.

The GPCP estimate of the trend in total rainfall for the selected regions, except for equatorial central Africa, is likely more reliable than CRU because GPCP takes

into account oceanic influences that are consistent with the decadal change of the large-scale circulation. The reduction of T10 in the maritime continent may reflect its location at the sinking branch of the anomalous Walker circulation. In contrast, the CRU data may reflect more local effects and less effects of the influence of the large-scale circulation changes. The strong fractional reductions for B5 rain shown in Figures 7(C) and (E) in CRU might be due to local effects and hence are not present in GPCP. Overall, the pronounced T10 relative changes in the two data sets are consistent in depicting a decadal shift in rainfall distribution, with regions of West Africa (Figure 7(A)), northern Australia (Figure 7(D)), and western equatorial South America (Figure 7(E)) falling under the influence of the rising branch, and equatorial Africa (Figure 7(B)), the maritime continent (Figure 7(C)), and eastern equatorial South America (Figure 7(F)) falling under the influence of the descending branch of an anomalous Walker circulation (Figure 7(D)). The results also agree with many previous observations of long-term trends in extreme precipitation in the climate record (Groisman *et al*., 2004; New *et al*., 2001; and others).

PHYSICAL INTERPRETATION

On the basis of the consistent shift in the PDF found in both GPCP and CMAP, we believe that both data sets may have captured the important physical processes that govern the long-term behavior of rainfall characteristics and redistribution in, and among, different parts of the rain spectrum, despite their discrepancy in trends in total tropical rain. In this section, we discuss a number of possibilities. Obviously, the physical processes discussed here are not definitive and need to be validated with further studies.

It is most interesting that the quasi-uniform pattern of the long-term trend in B5 rainfall over the ocean (Figure 6(A)) suggests that the increase may be thermodynamic in origin, possibly related to the increased precipitation efficiency for light rain owing to an increase in the sea-surface temperature (Lau and Wu, 2003). Recently, in a general circulation model (GCM) study of sensitivity of the atmospheric water cycle to cloud microphysical processes, Lau *et al*. (2005) showed that light, intermediate, and heavy rain events may be associated with greater proportion of warm (liquid phase), mixed-phase, and cold (ice phase) rain, respectively. They pointed out that the increased warm rain depletes low and middle clouds and deprives the upper atmosphere of available moisture for condensation by deep convection. This may be a reason for the reduction in intermediate rain (I25) found here, and is consistent with the large reduction of clouds as observed by the International Satellite Cloud Climatology Project (ISCCP), as well as an increase in the outgoing long wave radiation in the last two decades (Weilicki *et al*., 2002).

The substantial positive trend in the frequency of light rain and a possible induced reduction in cloudiness are important for the overall energy balance of the tropics because of the large area they occupy, i.e. greater than 40% of the tropical area, as estimated from GPCP. For the tropics as a whole, an increased cooling, through loss of heat to space due to the reduction in clouds stemming from an increase in warm rain over large regions, needs to be balanced by increased condensation heating elsewhere, generally over much smaller spatial scales because of the strong control by moisture convergence and local topographic uplifting. This may be the reason for the pronounced positive trend in intense rain (T10) located in deep convective cores of the ITCZ, SPCZ, and the Indian Ocean, as well as increased intermediate rain (I25) in the maritime continent and near the steep topography of the Andes (Figure 6(B)). Locally, when penetrative deep convection occurs, the clouds are pushed to higher altitudes, ice-phase rain dominates and mixed-phase rain reduces, and the converse happens in regions where mixed-phase rain dominates. In addition, anomalous rising motions from increased convection over the central Pacific and the Indian Ocean are known to drive the compensating subsidence, through Walker and Hadley type large-scale overturning, suppressing the rainfall over the maritime continent, northern South America, and the subtropics. These anomalous overturnings can be inferred from Figure 6(D). Hence, the inter-relationship in the trends for extreme light, heavy, and intermediate rains and their preferred locations may be understood in terms of the interplay of adjustment processes in the atmosphere water cycle, which involves dynamics, microphysics, and air-sea coupling, as manifested in the spatial redistribution of rainfall, long term change of tropical rain and cloud characteristics, as well as the trends in sea-surface temperature. It appears that such adjustment processes have also been partly captured in the recent coupled model simulations (Wang and Lau, 2005; Rotstayn and Lohmann, 2002; Meehl *et al*., 2000).

CONCLUSION

Using GPCP and CMAP pentad rainfall data, we have analyzed the trends of rainfall characteristics for the entire tropics for the period 1979–2003. Although the linear trend signals for total tropical rainfall differ considerably, the changes in the rainfall PDFs are qualitatively similar between the two data sets. Significant positive trends are found for light (bottom 5% by rain amount) and heavy rain (top 10%) categories, and negative trend is found for the intermediate rain (inter-quartile range) category. Light rains were found to have increased more or less uniformly over the tropical oceans in the last two decades. Amounts of heavy rain and their frequency of occurrence were found to be on the rise since the early 1980s in the cores of deep convection in the ITCZ, SPCZ, the Indian Ocean, and monsoon regions, but were found to be reduced over the maritime continent. Intermediate rains reduced over the warm pool regions and the ITCZ and

Published in 2006 by John Wiley & Sons, Ltd.

DOI: 10.1002/joc

SPCZ adjacent regions, but enhanced over the maritime continent. Both GPCP and CMAP show consistent and comparable spatial and temporal signals in linear trends for all three categories of rain. The linear trends and inter-relationships among the various rain components are found to be robust, in spite of the uncertainties in total rainfall. The shift in rainfall characteristics and the geographic redistribution of the amount of rain are determined by the interplay of planetary and cloud-scale adjustment processes of the entire tropical convection and large-scale circulation system.

Our results show that, while the atmospheric water cycle as measured by the long-term change in total tropical rainfall may be resilient to climate change because of large compensations, the structures of rain systems, especially the extreme rain events, may be more sensitive to a warming environment. The results are consistent with recent studies suggesting an increase in extreme weather events with global warming (Trenberth *et al*., 2003; Emannuel, 2005; Webster *et al*., 2005). This is also in general agreement with the analyses by Lau and Wu (2003), based on TRMM data, which show a substantial increase in precipitation efficiency of light warm rain as the sea-surface temperature increases. More modeling and observational studies need to be conducted to document the changing characteristics of rainfall, and associated structural changes in the global water cycle.

ACKNOWLEDGEMENTS

This work was supported by the Tropical Rainfall Measuring Mission (TRMM) of the NASA Science Mission Directorate. Drs. Hailan Wang and K. M. Kim conducted useful discussions and provided suggestions during the course of this work.

REFERENCES

Adler RF, Huffman GJ, Chang A, Ferraro R, Xie P-P, Janowiak J, Rudolf B, Shneider U, Curtis S, Bolvin D, Gruber A, Suskind J, Arkin P, Nelkin E. 2003. The version-2 global precipitation climatology project (GPCP) monthly precipitation analysis (1979-present). *Journal of Hydrometeorology* **4**: 1147–1167.

Allen MR, Ingram WJ. 2002. Constraints on future changes in climate and the hydrologic cycle. *Nature* **419**: 224–232.

Bosilovich MG, Schubert S, Walker G. 2005. Global changes of the water cycle intensity. *Journal of Climate* **18**: 1591–1607.

Emannuel K. 2005. Increasing destructiveness of tropical cyclones over the past 30 years. *Nature* **436**: 686–688.

Groisman PY, Knight RW, Easterling DR, Karl TR, Hegerl G, Razuvaev VN. 2004. Trends in intense precipitation in the climate record. *Journal of Climate* **18**: 1326–1350.

Intergovernmental Panel on Climate Change. 2001. Observed climate variability and change. In *Climate Change 2001: The Scientific Basis*, Houghton JT, Ding Y, Griggs DJ, Noguer M, van der Linden PJ, Dai X, Maskell K, Johnson CA (eds). Cambridge University Press: Cambridge, UK; 870 pp.

Karl T, Trenberth KE. 2003. Modern global climate change. *Science* **302**: 1719–1723.

Kumar A, Yang F, Goddard L, Schubert S. 2003. Differing trends in tropical surface temperatures and precipitation over land and oceans. *Journal of Climate* **17**: 653–664.

Lau K-M, Wu H-T. 2003. Warm rain processes over tropical oceans and climate implications. *Geophysical Research Letter* **30**: 2290–2294.

Lau K-M, Wu H-T, Sud YC, Walker GK. 2005. Effect of microphysical on tropical atmospheric hydrologic processes and intraseasonal variability. *Journal of Climate* **18**: 4731–4751.

Meehl GA, Zweiers F, Evans J, Knutson K, Mearns L, Whetton P. 2000. Trends in extreme weather and climate events: issues related to modeling extremes in projections of future climate change. *Bulletin of American Meteorological Society* **81**: 427–436.

Nesbitt SW, Zipser E, Kummerow C. 2004. An examination of version-5 rainfall estimates from the TRMM microwave imager, precipitation radar, and rain gauges on global, regional and storm scales. *Journal of Applied Meteorology* **43**: 1016–1036.

New M, Hulme M, Jones P. 2000. Representing twentieth-century space-time climate variability. Part II: development of 1901–1996 monthly grids of terrestrial surface climate. *Journal of Climate* **13**: 2217–2238.

New M, Todd M, Hulme M, Jones P. 2001. Precipitation measurements and trends in the twentieth century. *Journal of Climatology* **21**: 1899–1922.

Olson WS, Kummerow CD, Yang S, Petty GW, Tao W-K, Bell TL, Braun SA, Wang Y, Lang SE, Johnson DE, Chiu C. 2006. Precipitation and latent heating distributions from satellite passive microwave radiometry. Part I: Improved method and uncertainties. *Journal of Applied Meteorology & Climatology* **45**: 702–720.

Rotstayn L, Lohmann U. 2002. Tropical rainfall trends and the indirect aerosol effect. *Journal of Climate* **15**: 2103–2116.

Trenberth KE, Dai A, Rasmussen R, Parsons DB. 2003. The changing character of precipitation. *Bulletin of American Meteorological Society* **94**: 1205–1217.

Wang H, Lau K-M. 2006. Atmospheric hydrological cycle in the tropics in twentieth century coupled climate simulations. *International Journal of Climatology* **26**: 655–678.

Webster PJ, Holland GJ, Curry JA, Chang HR. 2005. Changes in tropical cyclone number, duration and intensity in a warming environment. *Science* **309**: 1844–1846.

Weilicki BA, Wong T, Allen RP, Slingo A, Kiehl JT, Soden BJ, Gordon CT, Miller AJ, Yang S-K, Randall DA, Robertson F, Susskind J, Jacobowitz H. 2002. Evidence for large decadal variability in the tropical mean radiative energy budget. *Science* **295**: 841–844.

Wilks DS. 1995. *Statistical Methods in the Atmospheric Sciences*. Academic Press: New York; 160–176.

Xie P-P, Janowiak JE, Arkin P, Ader R, Gruber A, Ferraro R, Juffman GJ, Curtis S. 2003. GPCP pentad precipitation analysis: An experimental dataset based on gauge observations and satellite estimates. *Journal of Climate* **16**: 2197–2214.

Yin X, Gruber A, Arkin P. 2004. Comparison of the GPCP and CMAP merged gauge-satellite monthly precipitation products for the period 1979–2001. *Journal of Hydrometeorology* **5**: 1207–1222.